Available online at www.sciencedirect.com
SCIENCE DIRECT®
Journal of Sound and Vibration 283 (2005) 875–890
JOURNAL OF SOUND AND VIBRATION
www.elsevier.com/locate/jsvi

Behavior of micropolar cubic crystal due to various sources

Rajneesh Kumar[a,*], Praveen Ailawalia[b]

[a]Department of Mathematics, Kurukshetra University, Kurukshetra 136–119, Haryana, India
[b]Department of Applied Sciences, I.E.E.T., Makhnumajra, Baddi, Distt. Solon, H.P., India

Received 21 November 2003; received in revised form 16 April 2004; accepted 17 May 2004
Available online 19 March 2005

Abstract

The response of a micropolar cubic crystal due to various sources acting at the free surface has been studied. The eigenvalue approach using integral transforms has been employed and the transforms have been inverted by using a numerical technique. The displacement, stress and microrotation components in the physical domain are obtained numerically. The results of displacement and stresses have been compared for micropolar cubic crystal and micropolar isotropic solid. The numerical results are illustrated graphically for a particular model.

1. Introduction

The theory of classical elasticity is based on the assumption that the microstructure of a material does not effect the descriptions of the mechanical behavior. However, material response to external stimuli depends on the motions of its inner structures. The discrepancies between the classical theory and the experiments are observed, indicating that the microstructure might be important. Some examples are: the stress concentrations in the neighborhood of holes, notches and cracks. Elastic vibrations characterized by high frequency and small wavelength, particularly in composites, materials containing laminates, fibers or grains.

Voigt [1] attempted to eliminate these discrepancies by suggesting that the interaction between the two particles of a body through an area element is transmitted not only by the action of a force

*Corresponding author.
E-mail addresses: rajneesh_kuk@rediffmail.com (R. Kumar), Praveen_2117@rediffmail.com (P. Ailawalia).

0022-460X/$ - see front matter © 2004 Elsevier Ltd. All rights reserved.
doi:10.1016/j.jsv.2004.07.001

vector but also by a moment (couple) vector. This led to the existence of couple stress in elasticity. Later Cosserat and Cosserat [2] explained a unified theory based on the concept of both linear displacement and rotation of every material particle during the deformation and is known as Cosserat theory of elasticity. In this theory, the deformation of the body is described by displacement vector and an independent rotation vector. The general relations and equations of the Cosserats theory have been derived by several authors (Kuvshinskii and Aero [25], Palmov [26]).

Eringen and Suhubi [3] and Suhubi and Eringen [4] introduced the theories of microelastic solids and microfluids in which the micromotions of the material particles contained in a macrovolume element with respect to its centroid are taken into account in an average sense. Materials affected by such micromotions and microdeformations are called micromorphic materials [5]. Eringen [6,7] developed theories for a subclass of micromorphic materials which are called micropolar media and these materials show microrotational effects and microrotational inertia. Here, the material particles in a volume element can undergo only rigid rotational motions about their center of mass. The motion described here is not only by a deformation but also by a micro-rotation giving six degrees of freedom. The interaction between two parts of a body is transmitted not only by a force but also a torque, resulting in asymmetric force stresses and couple stresses. Physically, solid propellant grains, polymeric materials and fiber glass are examples for such materials. The theory is expected to find applications in the treatment of mechanics of granular materials, composites fibrous materials and particularly microcracks and microfractures.

Following various methods, the elastic fields of various loadings, inclusion and inhomogeneity problems, and interaction energy of point defects and dislocation arrangement have been discussed extensively in the past. Generally all materials have elastic anisotropic properties which mean the mechanical behavior of an engineering material is characterized by the direction dependence. The formulation and solution of anisotropic problems is far more difficult and cumbersome than its isotropic counterpart, due to the large number of elastic constants involved in the calculation. In the recent years the elastodynamic response of anisotropic continuum has received the attention of several researchers. In particular, transversly isotropic and orthotropic materials, which may not be distinguished from each other in plane strain and plane stress, have been more regularly studied. The orthotropic material has the symmetry of its elastic properties with respect to two orthogonal planes, whereas a cubic material is a special case of orthotropic material that has the same properties along two axes and different properties along the third axis and is invariant to an additional change of coordinates. Kumar and Choudhary [8–10] discussed different types of problems in a micropolar orthotropic continua.

A wide class of crystals such as W, Si, Cu, Ni, Fe, Au, Al, etc., which are frequently used substances, belong to cubic materials. The cubic materials have nine planes of symmetry whose normals are on the three coordinate axes and on the coordinate planes making an angle $\pi/4$ with the coordinate axes. With the chosen coordinate system along the crystalline directions, the mechanical behavior of a cubic crystal can be characterized by four independent elastic constants A_1, A_2, A_3 and A_4.

To understand the crystal elasticity of a cubic material, Chung and Buessem [11] presented a convenient method to describe the degree of the elasticity anisotropy in a given cubic crystal. Later, Lie and Koehler [12] used a Fourier expansion scheme to calculate the stress fields caused by a unit force in a cubic crystal. Steeds [13] gave a complete discussion on the displacements, stresses and energy factors of the dislocations for two-dimensional anisotropic materials. Boulanger and Hayes [14] investigated inhomogeneous plane waves in cubic elastic materials. Bertram et al. [15] discussed generation of discrete isotropic orientation distributions for linear elastic cubic crystals. Kobayashi et al. [16] investigated anisotropy and curvature effects for growing crystals. Domanski and Jablonski [17] studied resonances of nonlinear elastic waves in cubic crystal. Destrade [18] considered the explicit secular equation for surface acoustic waves in monoclinic elastic crystals. Zhou and Ogawa [19] investigated elastic solutions for a solid rotating disk with cubic anisotropy. Minagawa et al. [20] discussed the propagation of plane harmonic waves in a cubic micropolar medium. Recently, Kumar and Rani [21] studied time harmonic sources in a thermally conducting cubic crystal. However, no attempt has been made to study source problems in micropolar cubic crystals.

The present problem is concerned with the determination of displacement, stress and microrotation components in a homogeneous micropolar cubic crystal half space due to mechanical sources. The problem has practical applications in the field of geomechanics, engineering, fiber-wound composites and laminated composite materials.

2. Formulation and solution of the problem

We consider a homogeneous, micropolar cubic crystal, elastic half-space in the undeformed state. We take the origin on the plane surface and y-axis normally into the medium, which is represented by $y \geqslant 0$. A normal point force is assumed to be acting at the origin of the rectangular Cartesian coordinate system (x, y, z). If we restrict our analysis to plane strain parallel to x–y plane with displacement vector $\vec{u} = (u_1, u_2, 0)$ and microrotation vector $\vec{\phi} = (0, 0, \phi_3)$ then the field equations and constitutive relations for such a medium in the absence of body forces and body couples can be written by following the equations given by Minagawa et al. [20] as

$$A_1 \frac{\partial^2 u_1}{\partial x^2} + A_3 \frac{\partial^2 u_1}{\partial y^2} + (A_2 + A_4) \frac{\partial^2 u_2}{\partial x \partial y} + (A_3 - A_4) \frac{\partial \phi_3}{\partial y} = \rho \frac{\partial^2 u_1}{\partial t^2}, \tag{1}$$

$$A_3 \frac{\partial^2 u_2}{\partial x^2} + A_1 \frac{\partial^2 u_2}{\partial y^2} + (A_2 + A_4) \frac{\partial^2 u_1}{\partial x \partial y} - (A_3 - A_4) \frac{\partial \phi_3}{\partial x} = \rho \frac{\partial^2 u_2}{\partial t^2}, \tag{2}$$

$$B_3 \nabla^2 \phi_3 + (A_3 - A_4) \left(\frac{\partial u_2}{\partial x} - \frac{\partial u_1}{\partial y} \right) - 2(A_3 - A_4)\phi_3 = \rho j \frac{\partial^2 \phi_3}{\partial t^2}, \tag{3}$$

$$t_{22} = A_2 \frac{\partial u_1}{\partial x} + A_1 \frac{\partial u_2}{\partial y}, \tag{4}$$

$$t_{21} = A_4 \left(\frac{\partial u_2}{\partial x} - \phi_3 \right) + A_3 \left(\frac{\partial u_1}{\partial y} + \phi_3 \right), \tag{5}$$

$$m_{23} = B_3 \frac{\partial \phi_3}{\partial y}. \tag{6}$$

In these relations, we have used the following notations: t_{22}, t_{21}—components of the force stress tensor, m_{23}—component of the couple stress tensor, u_1, u_2—components of displacement vector $\vec{u}$, ϕ_3—component of microrotation vector $\vec{\phi}$, A_1, A_2, A_3, A_4, B_3—characteristic constants of the material, ρ—the density and j—the microinertia .

Introducing the dimensionless variables defined by the expressions:

$$x' = \frac{\omega^*}{c_1}x, \quad y' = \frac{\omega^*}{c_1}y, \quad u_1' = \frac{\omega^*}{c_1}u_1, \quad u_2' = \frac{\omega^*}{c_1}u_2, \quad \phi_3' = \frac{A_1}{A_4}\phi_3,$$

$$\{t_{22}', t_{21}'\} = \frac{\{t_{22}, t_{21}\}}{A_1}, \quad m_{23}' = \frac{c_1}{B_3\omega^*}m_{23}, \quad t' = \omega^* t, \quad a' = \frac{\omega^*}{c_1}a, \tag{7}$$

where

$$\omega^{*2} = \frac{A_4 - A_3}{\rho j}, \quad c_1^2 = \frac{A_1}{\rho}. \tag{8}$$

Using Eq. (7), the system of Eqs. (1)–(3) reduce to (dropping the primes),

$$A_1\frac{\partial^2 u_1}{\partial x^2} + A_3\frac{\partial^2 u_1}{\partial y^2} + (A_2 + A_4)\frac{\partial^2 u_2}{\partial x \partial y} + \frac{A_4(A_3 - A_4)}{A_1}\frac{\partial \phi_3}{\partial y} = \rho c_1^2 \frac{\partial^2 u_1}{\partial t^2}, \tag{9}$$

$$A_3\frac{\partial^2 u_2}{\partial x^2} + A_1\frac{\partial^2 u_2}{\partial y^2} + (A_2 + A_4)\frac{\partial^2 u_1}{\partial x \partial y} - \frac{A_4(A_3 - A_4)}{A_1}\frac{\partial \phi_3}{\partial x} = \rho c_1^2 \frac{\partial^2 u_2}{\partial t^2}, \tag{10}$$

$$B_3\frac{A_4\omega^{*2}}{A_1 c_1^2}\nabla^2\phi_3 + (A_3 - A_4)\left(\frac{\partial u_2}{\partial x} - \frac{\partial u_1}{\partial y}\right) - 2\frac{A_4(A_3 - A_4)}{A_1}\phi_3 = \rho j \omega^{*2}\frac{A_4}{A_1}\frac{\partial^2 \phi_3}{\partial t^2}. \tag{11}$$

The initial and radiation conditions are given by

$$u_i(x,y,0) = \dot{u}_i(x,y,0) = 0, \quad i = 1,2,$$

$$\phi_3(x,y,0) = \dot{\phi}_3(x,y,0) = 0 \tag{12}$$

and

$$u_1(x,y,t) = u_3(x,y,t) = \phi_3(x,y,t) = 0 \quad \text{for } t>0, \text{ when } y \to \infty. \tag{13}$$

Applying Laplace transform with respect to time 't' defined by

$$\{\bar{u}_i(x,y,p), \bar{\phi}_3(x,y,p)\} = \int_0^\infty \{u_i(x,y,t), \phi_3(x,y,t)\}\mathrm{e}^{-pt}\,\mathrm{d}t, \quad i = 1,2 \tag{14}$$

and then Fourier transform with respect to 'x' defined by

$$\{\tilde{u}_i(\xi,y,p), \tilde{\phi}_3(\xi,y,p)\} = \int_{-\infty}^\infty \{\bar{u}_i(x,y,p), \bar{\phi}_3(x,y,p)\}\mathrm{e}^{\mathrm{i}\xi x}\,\mathrm{d}x, \quad i = 1,2 \tag{15}$$

on Eqs. (9)–(11) with the help of initial conditions, we obtain

$$\tilde{u}_1'' = b_{11}\tilde{u}_1 + e_{12}\tilde{u}_2' + e_{13}\tilde{\phi}_3', \tag{16}$$

$$\tilde{u}_2'' = b_{22}\tilde{u}_2 + e_{21}\tilde{u}_1' + b_{23}\tilde{\phi}_3, \tag{17}$$

$$\tilde{\phi}_3'' = b_{33}\tilde{\phi}_3 + e_{31}\tilde{u}_1' + b_{32}\tilde{u}_2, \tag{18}$$

where primes in Eqs. (16)–(18) represents differentiation with respect to y and

$$\begin{aligned}
&b_{11} = \frac{\rho c_1^2 p^2 + \xi^2 A_1}{A_3}, \quad b_{22} = \frac{\rho c_1^2 p^2 + \xi^2 A_3}{A_1}, \quad b_{23} = -\frac{\mathrm{i}\xi A_4(A_3 - A_4)}{A_1^2},\\
&b_{32} = \frac{\mathrm{i}\xi c_1^2 A_1(A_3 - A_4)}{\omega^{*2} A_4 B_3}, \quad b_{33} = \frac{1}{B_3}\left[\xi^2 B_3 + \rho j c_1^2 p^2 + 2(A_3 - A_4)\frac{c_1^2}{\omega^{*2}}\right],\\
&e_{13} = -\frac{A_4(A_3 - A_4)}{A_1 A_3}, \quad e_{21} = \frac{\mathrm{i}\xi(A_2 + A_4)}{A_1}, \quad e_{31} = \frac{A_1(A_3 - A_4)c_1^2}{A_4 B_3 \omega^{*2}},\\
&e_{12} = \frac{\mathrm{i}\xi(A_2 + A_4)}{A_3}.
\end{aligned} \tag{19}$$

Eqs. (16)–(18) may be written as

$$\frac{\mathrm{d}}{\mathrm{d}y} W(\xi, y, p) = A(\xi, p) W(\xi, y, p), \tag{20}$$

where

$$W = \begin{pmatrix} V \\ V' \end{pmatrix}, \quad A = \begin{pmatrix} O & I \\ A_1^* & A_2^* \end{pmatrix}, \quad V = \begin{pmatrix} \tilde{u}_1 \\ \tilde{u}_2 \\ \tilde{\phi}_3 \end{pmatrix},$$

$$A_1^* = \begin{pmatrix} b_{11} & 0 & 0 \\ 0 & b_{22} & b_{23} \\ 0 & b_{32} & b_{33} \end{pmatrix}, \quad A_2^* = \begin{pmatrix} 0 & e_{12} & e_{13} \\ e_{21} & 0 & 0 \\ e_{31} & 0 & 0 \end{pmatrix}, \tag{21}$$

O and I are, respectively, zero and identity matrix of order 3.

To solve Eq. (20), we assume

$$W(\xi, y, p) = X(\xi, p)\mathrm{e}^{qy}, \tag{22}$$

which leads to eigenvalue problem. The characteristic equation corresponding to matrix A is given by

$$|A - qI| = 0, \tag{23}$$

which on expansion provides us

$$q^6 + \lambda_1 q^4 + \lambda_2 q^2 + \lambda_3 = 0, \tag{24}$$

where

$$\lambda_1 = -(e_{12}e_{21} + e_{13}e_{31} + b_{11} + b_{22} + b_{33}),$$
$$\lambda_2 = e_{12}(e_{21}b_{33} - b_{23}e_{31}) + e_{13}(b_{22}e_{31} - e_{21}b_{32}) + b_{22}b_{33} - b_{23}b_{32} + b_{11}(b_{22} + b_{33}),$$
$$\lambda_3 = b_{11}(b_{23}b_{32} - b_{22}b_{33}). \tag{25}$$

The eigenvalues of the matrix A are characteristic roots of Eq. (24). The vectors $X(\xi,p)$ corresponding to the eigenvalues q_s can be determined by solving the homogeneous equation

$$[A - qI]X(\xi,p) = 0. \tag{26}$$

The set of eigenvectors $X_s(\xi,p)$, $s = 1,2\ldots6$ may be obtained as

$$X_s(\xi,p) = \begin{pmatrix} X_{s1}(\xi,p) \\ X_{s2}(\xi,p) \end{pmatrix}, \tag{27}$$

where

$$X_{s1}(\xi,p) = \begin{pmatrix} q_s \\ a_s \\ b_s \end{pmatrix}, \quad X_{s2}(\xi,p) = \begin{pmatrix} q_s^2 \\ a_s q_s \\ b_s q_s \end{pmatrix}, \quad q = q_s, \quad s = 1,2,3, \tag{28}$$

$$X_{j1}(\xi,p) = \begin{pmatrix} -q_j \\ a_j \\ b_j \end{pmatrix}, \quad X_{j2}(\xi,p) = \begin{pmatrix} q_j^2 \\ -a_j q_j \\ -b_j q_j \end{pmatrix}, \quad j = s+3, \quad q = -q_s, \quad s = 1,2,3 \tag{29}$$

and

$$a_s = \frac{b_{11}\,b_{23} - q_s^2(b_{23} + e_{21}\,e_{13})}{\nabla_s},$$
$$b_s = \frac{q_s^2\,e_{31} + a_s\,b_{32}}{q_s^2 - b_{33}},$$
$$\nabla_s = q_s^2\,e_{13} + e_{12}\,b_{23} - b_{22}\,e_{13}. \tag{30}$$

The solution of Eq. (22) is given by

$$W(\xi,y,p) = \sum_{s=1}^{3}[D_s X_s(\xi,p)\ \exp(q_s y) + D_{s+3}\,X_{s+3}(\xi,p)\ \exp(-q_s y)]. \tag{31}$$

The transformed displacements and microrotation satisfying the radiation conditions (13) are given by

$$\tilde{u}_1 = -q_1 D_4\ \exp(-q_1 y) - q_2 D_5\ \exp(-q_2 y) - q_3 D_6\ \exp(-q_3 y),$$
$$\tilde{u}_2 = a_1 D_4\ \exp(-q_1 y) + a_2 D_5\ \exp(-q_2 y) + a_3 D_6\ \exp(-q_3 y),$$
$$\tilde{\phi}_3 = b_1 D_4\ \exp(-q_1 y) + b_2 D_5\ \exp(-q_2 y) + b_3 D_6\ \exp(-q_3 y). \tag{32}$$

3. Boundary conditions and application

Mechanical sources acting on the surface of the half-space: The boundary conditions in this case are

$$t_{22} = -F\psi(x)\delta(t), \quad t_{21} = m_{23} = 0, \tag{33}$$

where $\delta(t)$ is Dirac delta function, F is the magnitude of force applied and $\psi(x)$ specify the vertical load distributed function along x-axis.

Using Eqs. (7) and then applying Laplace and Fourier transforms from Eqs. (14) and (15) on system of Eqs. (33) and with the help of Eqs. (32), we get the transformed displacement, microrotation and stresses as

$$\tilde{u}_2 = -\frac{F}{\Delta}\left[a_1\Delta_1' \,\mathrm{e}^{-q_1 y} - a_2\Delta_2' \,\mathrm{e}^{-q_2 y} + a_3\Delta_3' \,\mathrm{e}^{-q_3 y}\right], \tag{34}$$

$$\tilde{t}_{22} = -\frac{F}{\Delta}\left[r_1\Delta_1' \,\mathrm{e}^{-q_1 y} - r_2\Delta_2' \,\mathrm{e}^{-q_2 y} + r_3\Delta_3' \,\mathrm{e}^{-q_3 y}\right], \tag{35}$$

$$\tilde{m}_{23} = \frac{FA_4}{A_1\Delta}\left[b_1 q_1\Delta_1' \,\mathrm{e}^{-q_1 y} - b_2 q_2\Delta_2' \,\mathrm{e}^{-q_2 y} + b_3 q_3\Delta_3' \,\mathrm{e}^{-q_3 y}\right], \tag{36}$$

where

$$\Delta = \frac{1}{\tilde{\psi}(\varphi)}\,[r_1\Delta_1' - r_2\Delta_2' + r_3\Delta_3'], \quad \Delta_{1,2,3}' = \tilde{\psi}(\varphi)\,[s_{2,1,1}\, b_{3,3,2}\, q_{3,3,2} - s_{3,3,2}\, b_{2,1,1}\, q_{2,1,1}],$$
$$r_\Theta = q_\Theta\left(\mathrm{i}\xi\frac{A_2}{A_1} - a_\Theta\right), \quad s_\Theta = -\mathrm{i}\xi a_\Theta A_4 + q_\Theta^2 A_3 + \frac{A_4}{A_1}(A_3 - A_4)b_\Theta,$$
$$\Theta = 1,2,3. \tag{37}$$

3.1. Concentrated normal force

In order to determine displacements, microrotation and stresses due to concentrated normal force described as Dirac delta function $\psi(x) = \delta(x)$ must be used. The Fourier transform of $\psi(x)$ with respect to pair (x, ξ) will be $\tilde{\psi}(\xi) = 1$.

3.2. Uniformly distributed force

The solution due to uniformly distributed force applied on the half-space is obtained by setting

$$\psi(x) = \begin{cases} 1 & \text{if} \quad |x| \leqslant a, \\ 0 & \text{if} \quad |x| > a, \end{cases}$$

in Eqs. (33). The Fourier transform with respect to the pair (x, ξ) for the case of a uniform strip load of unit amplitude and width 2a applied at the origin of the coordinate system $(x = y = 0)$ in dimensionless form after suppressing the primes becomes

$$\tilde{\psi}(\xi) = \left[2\,\sin\left(\frac{\xi c_1 a}{\omega^*}\right)\xi\right], \quad \xi \neq 0. \tag{38}$$

3.3. Linearly distributed force

The solution due to linearly distributed force is obtained by substituting

$$\psi(x) = \begin{bmatrix} 1 - \frac{|x|}{a} & if & |x| \leqslant a, \\ 0 & if & |x| > a. \end{bmatrix} \tag{39}$$

The Fourier transform in case of linearly distributed force applied at the origin of the system in dimensionless form are

$$\tilde{\psi}(\varphi) = \frac{2[1 - \cos(\xi c_1 a/\omega^*)]}{\xi^2 c_1 a/\omega^*}. \tag{40}$$

The expressions for displacement, force stress and couple stress may be obtained as in Eqs. (34)–(36), by replacing $\tilde{\psi}(\varphi)$ by 1, $\left[2\,\sin(\xi c_1 a/\omega^*)/\xi\right]$ and $2[1 - \cos(\xi c_1 a/\omega^*)]/\xi^2 c_1 a/\omega^*$ in case of concentrated force, uniformly distributed force and linearly distributed force, respectively.

Particular case: Taking $A_1 = \lambda + 2\mu + K$, $A_2 = \lambda$, $A_3 = \mu + K$, $A_4 = \mu$, $B_3 = \gamma$, we obtain the corresponding expressions for the micropolar isotropic medium. These results tally with the one if we solve the problem in micropolar isotropic medium.

4. Inversion of the transform

The transformed displacements and stresses are functions of y, the parameters of Laplace and Fourier transforms p and ξ, respectively, and hence are of the form $\tilde{f}(\xi, y, p)$. To get the function in the physical domain, first we invert the Fourier transform using

$$\begin{aligned}\bar{f}(x, y, p) &= \frac{1}{2\pi}\int_{-\infty}^{\infty} e^{-i\xi x}\tilde{f}(\xi, y, p)\,d\xi \\ &= \frac{1}{\pi}\int_{0}^{\infty}\{\cos(\xi x)f_e - i\,\sin(\xi x)f_o\}\,d\xi,\end{aligned} \tag{41}$$

where f_e and f_o are even and odd parts of the function $\tilde{f}(\xi, y, p)$, respectively. Thus, expressions (34)–(36) give us the transform $\bar{f}(x, y, p)$ of the function $f(x, y, t)$.

Following Honig and Hirdes [22] the Laplace transform function $\bar{f}(x, y, p)$ can be inverted to $f(x, y, t)$.

The last step is to evaluate the integral in Eq. (41). The method for evaluating this integral is given by Press et al. [23] and which involves the use of Rhomberg's integration with adaptive step size. This, also uses the results from successive refinement of the extended trapezoidal rule followed by extrapolation of the results to the limit when the step size tends to zero.

5. Numerical results and discussions

For numerical computations, we take the following values of relevant parameters for micropolar cubic crystal as

$$A_1 = 13.97 \times 10^{10}\,\text{dyn/cm}^2, \quad A_3 = 3.2 \times 10^{10}\,\text{dyn/cm}^2,$$
$$A_2 = 13.75 \times 10^{10}\,\text{dyn/cm}^2, \quad A_4 = 2.2 \times 10^{10}\,\text{dyn/cm}^2, \quad B_3 = 0.056 \times 10^{10}\,\text{dyn}.$$

For the comparison with micropolar isotropic solid, following Gauthier [24], we take the following values of relevant parameters for the case of aluminium epoxy composite as

$$\rho = 2.19\,\text{g/cm}^3, \quad \lambda = 7.59 \times 10^{10}\,\text{dyn/cm}^2, \quad \mu = 1.89 \times 10^{10}\,\text{dyn/cm}^2,$$
$$K = 0.0149 \times 10^{10}\,\text{dyn/cm}^2, \quad \gamma = 0.0268 \times 10^{10}\,\text{dyn}, \quad j = 0.00196\,\text{cm}^2.$$

The values of normal displacement $U_2 = (u_2/F)$, normal force stress $T_{22} = (t_{22}/F)$ and tangential couple stress $M_{23} = (m_{23}/F)$ for a micropolar cubic crystal (MCC) and micropolar isotropic solid (MIS) have been studied at $t = 0.1$, 0.2 and 0.5 and the variations of these components with distance x have been shown by (a) solid line (——) for MCC and dashed line (--------) for MIS at $t = 0.1$, (b) solid line with centered symbol (x—x—x) for MCC and dashed line with centered symbol (x- - -x- - -x) for MIS at $t = 0.2$ and (c) solid line with centered symbol (∘—∘—∘) for MCC and dashed line with centered symbol (∘- - -∘- - -∘) for MIS at $t = 0.5$. These variations are shown in Figs. 1–9. The comparison between a cubic crystal and an isotropic solid are shown. The computations are carried out for $y = 1.0$ in the range $0 \leqslant x \leqslant 10.0$.

6. Discussions for various cases

6.1. Concentrated normal force

The variations of normal displacement and normal force stress are opposite in nature. It is observed from Fig. 1 that the values of normal displacement, very close to the point of application of source, are more for MCC at a particular time but the values for both MCC and MIS decreases with increase in time.

The variations of normal force stress are more oscillatory for MCC as compared to MIS. These variations depicted in Fig. 2, decreases with increase in horizontal distance. The variations of normal force stress for both MCC and MIS are quite close to each other in the initial range at $t = 0.1$. However, the difference in variations of normal force stress among both the solids increases with increase in time.

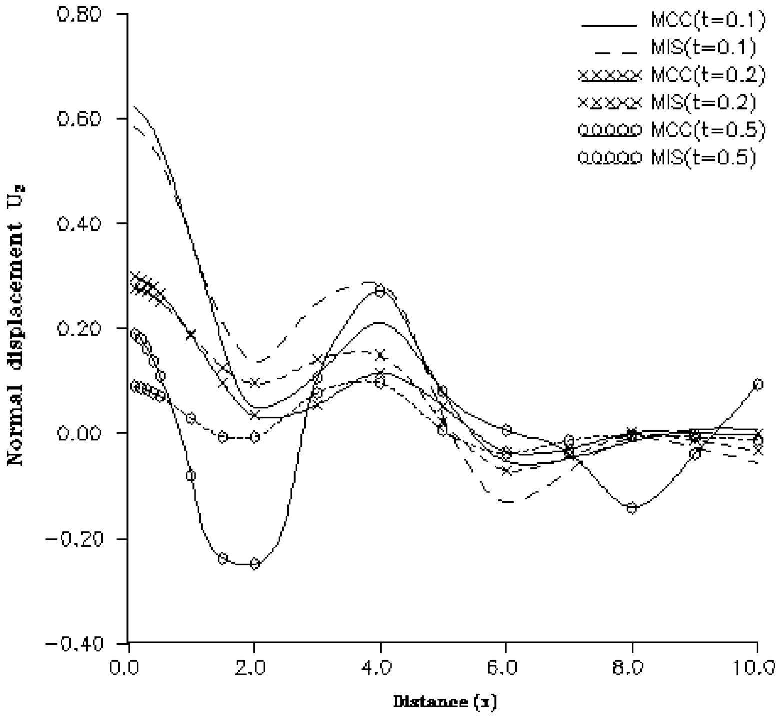

Fig. 1. Variation of normal displacement $U_2(=u_{22}/F)$ with horizontal distance x for concentrated force.

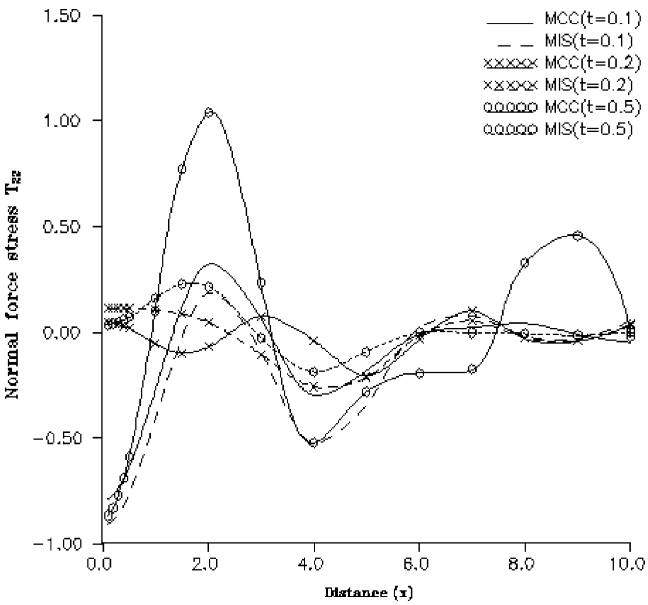

Fig. 2. Variation of normal force stress $T_{22}(=t_{22}/F)$ with horizontal distance x for concentrated force.

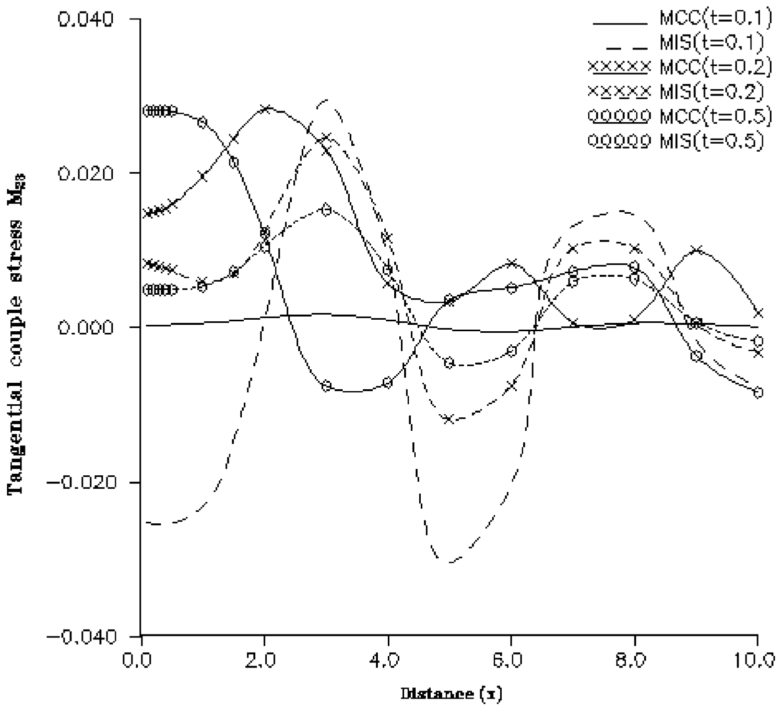

Fig. 3. Variation of tangential couple stress $M_{23}(=m_{23}/F)$ with horizontal distance x for concentrated force.

The values of tangential couple stress for MCC at $t = 0.1$ lies in a very short range. Also the values for MCC, very close to the point of application of source, increases with increase in time. The magnitude of oscillations of tangential couple stress decreases with increase in horizontal distance x. These variations of tangential couple stress are shown in Fig. 3.

6.2. Uniformly distributed force

The values of normal displacement for MCC lies in a short range as compared to the values for MIS. The magnitude of oscillations of normal displacement for MIS decreases with increase in time as shown in Fig. 4. Similar to the nature for normal displacement, the values of normal force stress and tangential couple stress are less for MCC in comparison to the values for MIS. It is observed from Fig. 5 that the values of normal force stress for both MCC and MIS rises initially but the rise in values is more sharp for MIS. The values of normal force stress for MIS at $t = 0.1$ and $t = 0.2$ have been demagnified by 10.

It is quite interesting to see that while the values of tangential couple stress for MCC lies in a very short range, the values for MIS, very close to the point of application of source, increases with time. The variations of tangential couple stress for uniformly distributed force are shown in Fig. 6. To compare the variations of the two solids the values of tangential couple stress for MIS at $t = 0.1,\ 0.2\, and\, 0.5$ have been demagnified by 10.

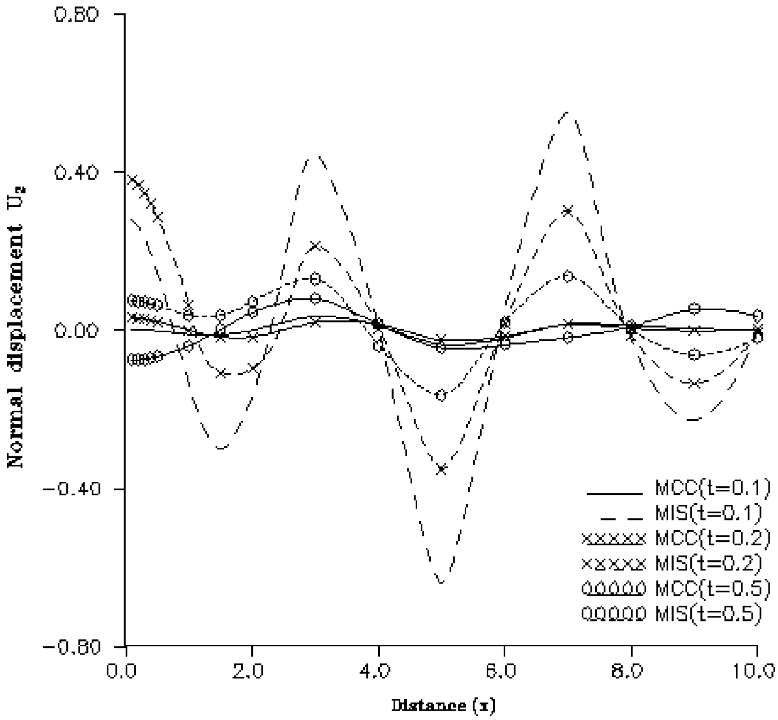

Fig. 4. Variation of normal displacement $U_2(=u_{22}/F)$ with horizontal distance x for uniformly distributed force.

6.3. Linearly distributed force

The variations of normal displacement and normal force stress for both MCC and MIS and for $t=0.1$ and $t=0.2$ are similar in nature. The nature of normal displacement and normal force stress among themselves are opposite in nature. The values of normal displacement decreases with increase in distance x whereas the values of normal force stress increases. It is evident from Figs. 7 and 8 depicting the variations of normal displacement and normal force stress respectively that contrary to the variations at $t=0.1$ and $t=0.2$, the variations at $t=0.5$ are oscillatory in nature.

The values of tangential couple stress for MIS are less as compared to the values for MCC. The values of tangential couple stress for MCC increases with increase in distance x but the values for MIS first increases and then decreases with increase in horizontal distance. The variations of tangential couple stress shown in Fig. 9 shows that the values for both MCC and MIS converges to zero as the source moves away from the point of application. Also the variations for both solids are compared after magnifying the values for MIS by 10.

7. Conclusion

The properties of a body depend largely on the direction of symmetry. The variations of all the quantities are oscillatory in nature when concentrated force or uniformly distributed force is

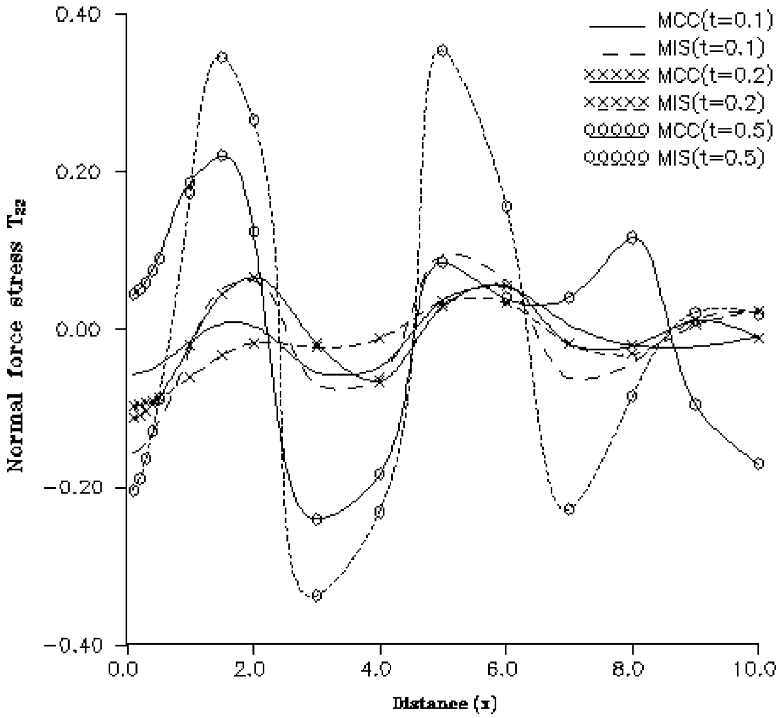

Fig. 5. Variation of normal force stress $T_{22}(= t_{22}/F)$ with horizontal distance x for uniformly distributed force.

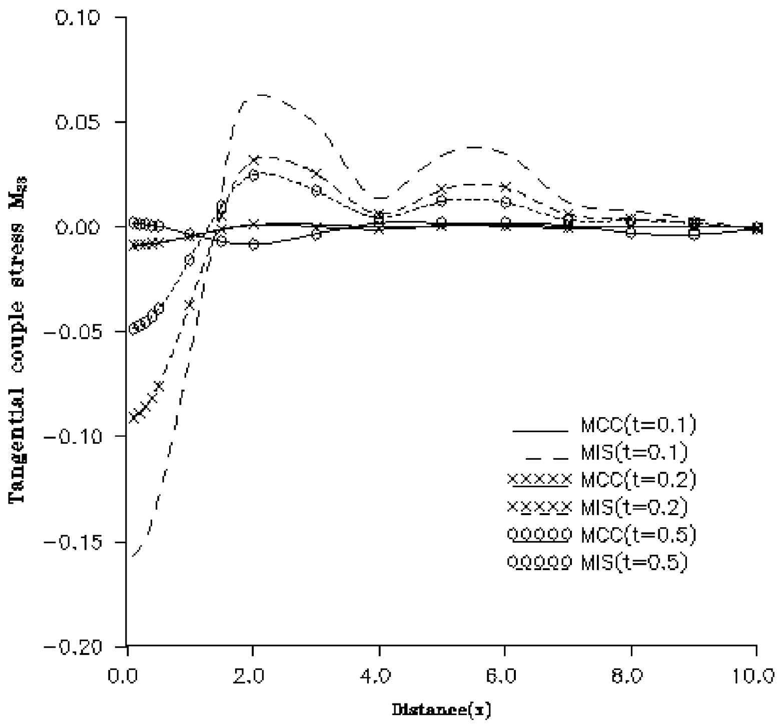

Fig. 6. Variation of tangential couple stress $M_{23}(= m_{23}/F)$ with horizontal distance x for uniformly distributed force.

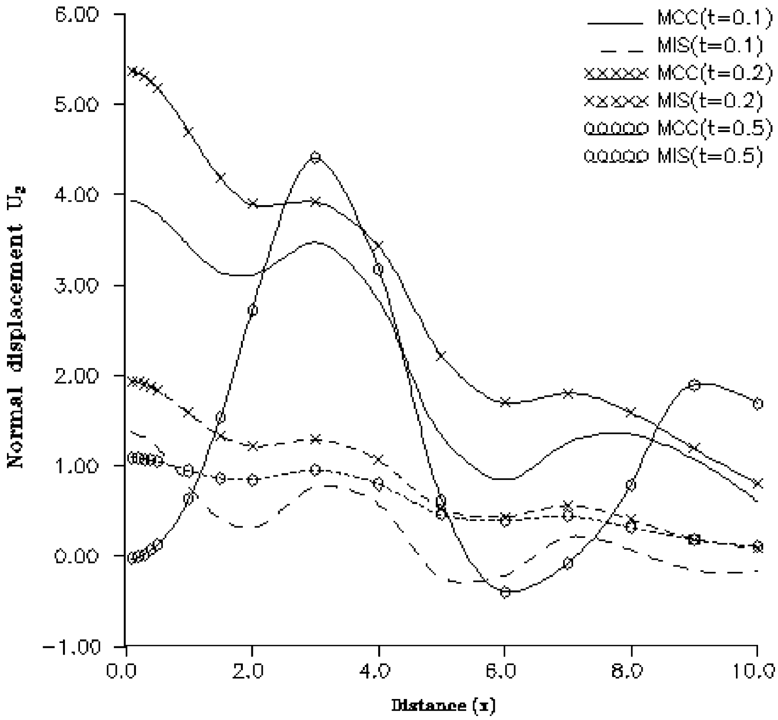

Fig. 7. Variation of normal displacement $U_2(=u_{22}/F)$ with horizontal distance x for linearly distributed force.

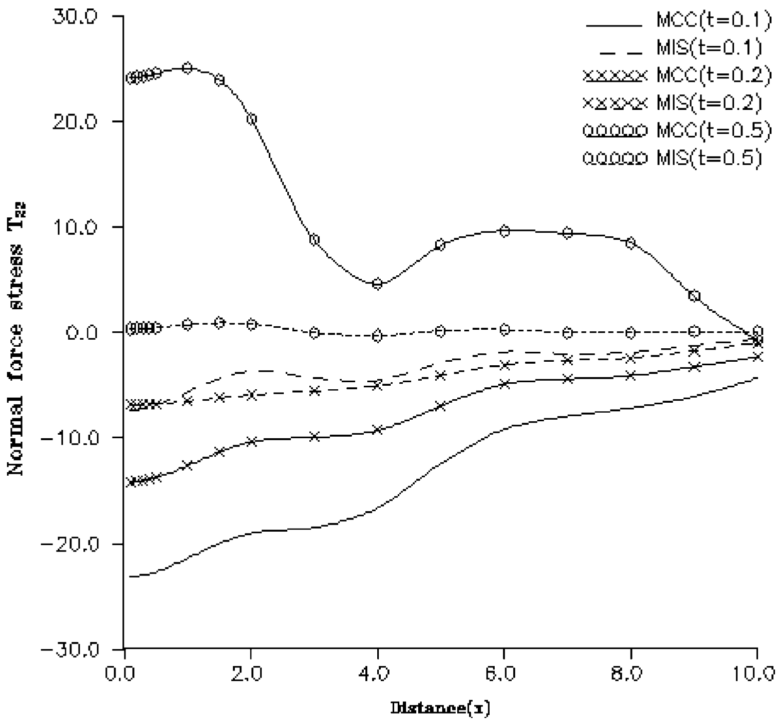

Fig. 8. Variation of normal force stress $T_{22}(=t_{22}/F)$ with horizontal distance x for linearly distributed force.

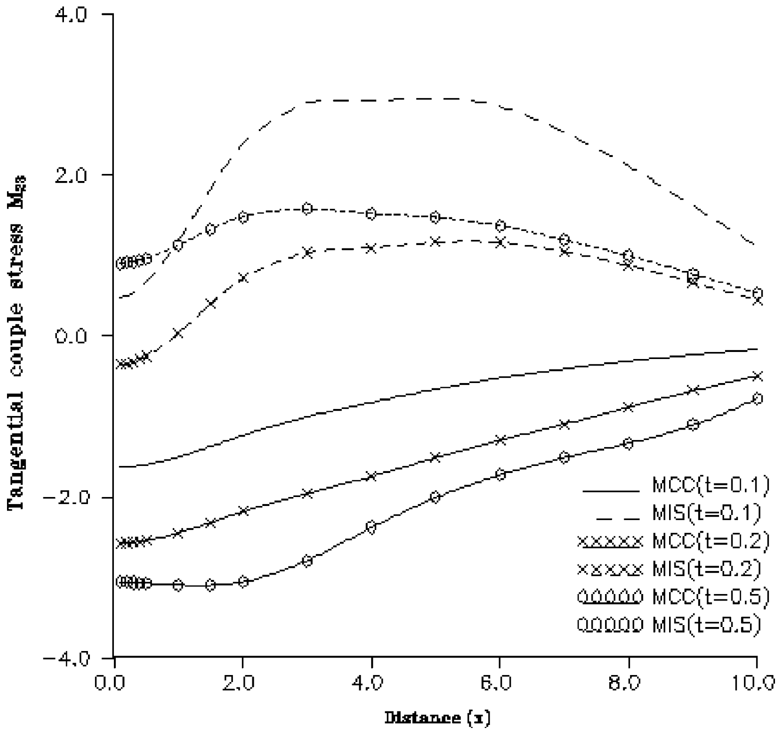

Fig. 9. Variation of tangential couple stress $M_{23}(=m_{23}/F)$ with horizontal distance x for linearly distributed force.

applied on the surface. Also the values of normal force stress and tangential couple stress are large for MIS when uniformly distributed force is applied but on the application of linearly distributed force, the values of tangential couple stress for MIS decreases in comparison to the values for MCC.

References

[1] W. Voigt, Theoretische studien uber die Elastizitatverhaltnisse der Kristalle Abhanclbungen der Königlichen Gesellschaft zu Göttingen 34 (1887).

[2] E. Cosserat, F. Cosserat, *Theories des corpc deformables*, A. Hermann, Paris, 1909.

[3] A.C. Eringen, E.S. Suhubi, Non linear theory of simple microelastic solids I, *International Journal of Engineering Science* 2 (1964) 189–203.

[4] E.S. Suhubi, A.C. Eringen, Non linear theory of microelastic solids II, *International Journal of Engineering Science* 2 (1964) 389–404.

[5] A.C. Eringen, Mechanics of micromorphic materials, *Proceedings XI. International Congress of Applied Mechanics*. Springer, Berlin, 1965.

[6] A.C. Eringen, Linear theory of micropolar elasticity, *Journal of Mathematics and Mechanics* 15 (1966) 909–923.

[7] A.C. Eringen, Theory of micropolar fluids, *Journal of Mathematics and Mechanics* 16 (1966) 1–18.

[8] R. Kumar, S. Choudhary, Influence and Green's function for orthotropic micropolar continua, *Archives of Mechanics* 54 (2002) 185–198.

[9] R. Kumar, S. Choudhary, Dynamical behavior of orthotropic micropolar elastic medium, *Journal of vibration and Control* 8 (2002) 1053–1069.
[10] R. Kumar, S. Choudhary, Response of orthotropic micropolar elastic medium due to various sources, *Meccanica* 38 (2003) 349–368.
[11] D.H. Chung, W.R. Buessem, The elastic anisotropy of crystals, *Journal of Applied Physics* 38 (5) (1967) 2010–2012.
[12] K-H.C. Lie, J.S. Koehler, The elastic stress field produced by a point force in a cubic crystal, *Advances in Physics* 17 (1968) 421–478.
[13] J.W. Steeds, *Introduction to Anisotropic Elasticity Theory of Dislocations*, Clarendon Press, Oxford, 1973.
[14] P. Boulanger, M. Hayes, Special inhomogeneous plane waves in cubic elastic materials, *Zeitschrift für angewandte Mathematik und Physik* 51 (2000) 1031–1038.
[15] A. Bertram, T. Bohlke, N. Gaffke, B. Heiligers, R. Offinger, On the generation of discrete isotropic orientation distributions for linear elastic cubic crystals, *Journal of Elasticity* 58 (3) (2000) 233–248.
[16] R. Kobayashi, Y. Giga, On anisotropy and curvature effects for growing crystals, *Japan Journal of Industrial and Applied Mathematics* 18 (2) (2001) 207–230.
[17] W. Domanski, T. Jablonski, On resonances of nonlinear elastic waves in a cubic crystal, *Archieves of Mechanics* 53 (2) (2001) 91–104.
[18] M. Destrade, The explicit secular equation for surface acoustic waves in monoclinic elastic crystals, *Journal of Acoustical Society of America* 109 (4) (2001) 1398–1402.
[19] F. Zhou, A. Ogawa, Elastic solutions for a solid rotating disk with cubic anisotropy, *ASME Journal of Applied Mechanics* 69 (2002) 81–83.
[20] S. Minagawa, K. Arakawa, M. Yamada, Dispersion curves for waves in a cubic micropolar medium with reference to estimations of the material constants for diamond, *Bulletin of Japan Society of Mechanical Engineers* 24 (187) (1981) 22–28.
[21] R. Kumar, L. Rani, Elastodynamics of time harmonic sources in a thermally conducting cubic crystal, *International Journal of Applied Mechanics and Engineering* 8 (4) (2003) 637–650.
[22] G. Honig, V. Hirdes, A method for the numerical inversion of the Laplace transform, *Journal of Computational and Applied Mathematics* 10 (1984) 113–132.
[23] W.H. Press, S.A. Teukolsky, W.T. Vellerling, B.P. Flannery, *Numerical Recipes*, Cambridge University Press, Cambridge, 1986.
[24] R.D. Gauthier, Experimental investigations on micropolar media, in: O. Brulin, R.K.T. Hsieh (Eds.), *Mechanics of Micropolar Media*, World Scientific, Singapore, 1982.
[25] E.V. Kuvshinskii, E.L. Aero, Continuum theory of asymmetric elasticity, *Fizika Tverdogo Tele* 5 (1963) 2592–2598.
[26] M.A. Palmov, Fundamental equations of theory of asymmetric elasticity, *Prikladnaya Matematika i Mekhanika* 28 (1964) 401–409.